Biophysical Chemistry 136 (2008) 128–135

Contents lists available at ScienceDirect

Biophysical Chemistry

journal homepage: http://www.elsevier.com/locate/biophyschem

Distribution and favorable binding sites of pyrroloquinoline and its analogues in a lipid bilayer studied by molecular dynamics simulations

Alexander Kyrychenko [a,*,1], Jacek Waluk [b]

[a] Institute for Chemistry, V.N. Karazin Kharkov National University, 4 Svobody Sq., 61077, Kharkov, Ukraine
[b] Institute of Physical Chemistry, Polish Academy of Sciences, Kasprzaka 44/52, 01-224 Warsaw, Poland

ARTICLE INFO

Article history:
Received 20 April 2008
Received in revised form 22 May 2008
Accepted 22 May 2008
Available online 16 June 2008

Keywords:
Molecular dynamics simulation
Lipid bilayer
Fluorescence probe
Proton transfer

ABSTRACT

The distribution of 1*H*-pyrrolo[3,2-*h*]quinoline (PQ), 11*H*-dipyrido[2,3-*a*]carbazole (PC) and 7-azaindole (7AI) at a water/membrane interface has been investigated by molecular dynamics (MD) simulations. The MD study focused on favorable binding sites of the azaaromatic probes across a dipalmitoylphosphatidylcholine (DPPC) bilayer. Our simulations show that PQ and PC are preferably accommodated at the hydrocarbon core of the bilayer below the glycerol moiety. In addition, it is found that the hydrophobic aromatic parts of the probes are located inside a more ordered region of DPPC, consisting of hydrophobic lipid chains. In contrast to PQ and PC, 7AI is characterized by a broad distribution between a DPPC interface and water, so that the three preferable binding sites are found across a water/membrane interface. It is found that in the sequence 7AI–PQ–PC, due to the increase of the number of aromatic rings and, hence, the hydrophobic character of the probes, the depth of the probe localization is gradually shifted deeper inside the hydrocarbon core of the bilayer. We found that the probe–lipid hydrogen-bonding contributes weakly to the favorable localizations of the azaaromatic probes inside the DPPC bilayer, so that the probe localization is mainly driven by electrostatic dipole–dipole and van der Waals interactions.

1. Indroduction

Azaaromatic compounds composed of pyrrole, indole, and quinoline moieties reveal an interesting phenomenon of solvent-catalyzed excited-state tautomerization [1]. The electronic excitation in such systems induces remarkable and cooperative acid–base changes, occurring on opposite parts of an electronically excited chromophore. These changes introduce a driving force for proton translocation between spatially-separated hydrogen bond donor (*D*) and acceptor (*A*) groups. Despite of favorable energetics, such phototautomerization cannot, however, occur directly due to an unfavorable *D–A* spatial separation. On the other hand, in the presence of some appropriate protic solvents, bifunctional hydrogen hydrogen bond *D–A* compounds are able to form cyclic intermolecular H-bonded complexes, in which solvent molecules act as wires connecting the *D–A* centers. In such H-bonded solute–solvent complexes, solvent-assisted excited-state proton transfer becomes possible. Fig. 1 shows the molecular structure of representative examples of bifunctional *D–A* azaaromatics which reveal H-bond-mediated tautomerization in the excited-state [2–10]: 1*H*-pyrrolo[3,2-*h*]quinoline (PQ) and 11*H*-dipyrido[2,3-*a*]carbazole (PC). 7-Azaindole (7AI), one of the best known examples of bifunctional compounds which show solvent-assisted tautomerization [11,12], is also included.

One of the most remarkable features of the formation of a cyclic H-bonded solute–solvent complex is the appearance of an additional, red-shifted fluorescence band in the emission spectra recorded in alcohol and water solutions. This emission has been attributed to the fluorescence of a tautomeric form, first reported by Kasha and coworkers for 7AI in alcohol complexes [11,12]. It has also been reported for several other hydrogen-bonded host–guest systems [13]. Other well-documented examples of solvent-assisted proton transfer systems include 3-hydroxyisoquinoline [14] and 7-hydroxyquinolines [15–21]. The hydrogen-bond-controlled excited-state behavior has also been observed for 2-(2′-pyridyl) indoles in alcohols [22-24].

The proton transfer photoreactivity of bifunctional *D–A* azaaromatic compounds, such as PQ and 7AI, has been found to be strongly dependent on the stoichiometry, structure and length of the hydrogen-bonded bridge [6–10,13,25,26]. Therefore, upon electronic excitation azaaromatic compounds of this series reveal remarkable sensitivity to the presence of protic impurities, such as alcohols or water [27–29]. The hydrogen-bonding-dependent photophysics makes these compounds very promising candidates for fluorescent probes and sensors of water content and penetration depth of water molecules in biomembranes or micelles [20,21,30,31]. The tuning of signaling features of such probes is predominantly connected to cyclic hydrogen-bonding with a single protic molecule, resulting in the

* Corresponding author. Tel.: +380 57 707 5335.
E-mail address: alexander.v.kyrychenko@univer.kharkov.ua (A. Kyrychenko).
[1] Present address: University of Kansas Medical Center, Department of Biochemistry and Molecular Biology, MS 3030, 3901 Rainbow Blvd., Kansas City, KS 66160-7421, USA.

0301-4622/$ – see front matter © 2008 Elsevier B.V. All rights reserved.
doi:10.1016/j.bpc.2008.05.006

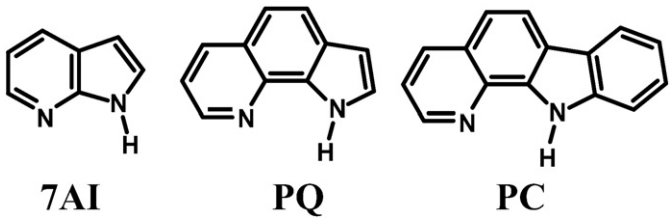

Fig. 1. Structure of 1*H*-pyrrolo[3,2-*h*]quinoline (PQ), 11*H*-dipyrido[2,3-*a*]carbazole (PC) and 7-azaindole (7AI).

appearance of a second long-wavelength band in the emission spectrum. Therefore, specific hydrogen bonding may switch the fluorescence behavior of these systems between the single and double emission band regimes. The operating principle of such "off–on" fluorescence signaling is schematically shown in Fig. 2. In addition to solvent-assisted proton transfer systems, interesting examples of fluorescent probes are provided by compounds which reveal an intramolecular excited-state proton transfer (ESIPT) reaction [32,33]. The detailed knowledge of a favorable location of a fluorescent probe inside a membrane is, therefore, important for designing new compounds while exploring structural and dynamic properties at specific depths within a membrane [34–36].

Molecular dynamics (MD) simulations are widely used to examine processes of location and distribution of small hydrophobic/hydrophilic solutes in phospholipid bilayers with atomic details [37–39]. This approach has also been frequently employed to study biosorption and permeation of biologically relevant drug molecules across cell membranes [40,41]. These theoretical approaches have proven to be very powerful in determining, with atomic resolution, the partitioning behavior of solutes inside membranes that are often difficult to study experimentally. In addition, MD simulations have been used as a supplementary tool for experimental, mainly fluorescence and NMR, studies of the distribution and orientation of aromatic hydrocarbon probes in various lipid environments. Recently, the combination of solid-state ^{2}H NMR spectroscopy and MD methods has been used to determine the alignment and localization of pyrene in 1-palmitoyl-2-oleoyl-phosphatidylcholine (POPC) [42] and DPPC [43] bilayers. 1,6-Diphenyl-1,3,5-hexatriene (DPH) has often been applied as a fluorescent probe for studying, using both spectroscopy and MD methods [44,45], rotational and lateral diffusion processes in lipid bilayers. A number of other studies have employed a variety of biased simulation techniques to calculate the partitioning behavior of probes inside model membranes. Furthermore, constraint-based MD studies have been carried out to examine the diffusion and partition processes of a series of small solutes across DPPC bilayers [46]. Lidocaine penetration into a dimyristoylphosphatidylcholine (DMPC) bilayer has recently been studied by computer simulations [47]. Among other MD methods, an umbrella sampling technique has been used to investigate the distribution of a volatile anesthetic, halothane, in dioleoylphosphatidylcholine (DOPC) bilayers, derived from free-energy profile calculations [48,49].

As a first step toward experimental investigating the partitioning behavior of PQ and PC inside a model lipid membrane, we have performed a set of unbiased all-atom MD simulations, designed to provide insight into the distribution and favorable binding sites of the probe molecules within a DPPC bilayer. The main goal of our MD study was to rationalize the distribution of the azaaromatic compounds (Fig. 1) in a model lipid bilayer. These findings help us to understand which regions within a lipid bilayer are most favored by the probes. 7AI was used as a structurally similar probe for which a number of well-documented experimental studies are available [50–53]. It has been demonstrated that tryptophan and indole probes distribute preferentially to the lipid–water interface of membranes, so that the probes are found to be in easy contact with water [50–53]. The diversity of chemical properties, in particular relative hydrophobicity and molecular dipole moment, suggest that, among PQ, PC and 7AI, their partitioning and favorable location inside membranes is expected to differ significantly. The MD simulations allow us to explore the most favorable binding sites for these probes within a DPPC bilayer. Preferable hydrogen bonding of the probes with interfacial water was also studied as a function of the probe location across the bilayer. In the following sections we will briefly describe the MD simulation methodology. Simulation results on the distribution of PQ, PC and 7AI molecules in the DPPC bilayer will be analyzed and compared with available experimental and theoretical results for structurally similar azaaromatic probes, consisting of pyrrole and pyridine moieties. Possible applications of these fluorescent molecules for studying the structural properties of lipid bilayers and in monitoring the water content in membranes will be discussed.

2. System setup and MD simulation details

A simulated lipid bilayer consists of 128 dipalmitoylphosphatidylcholine (DPPC) lipids (64 per leaflet) surrounded by 4310 water molecules. A lipid-to-water ratio is about 1:33, so that a bilayer is simulated in the fully hydrated state. In the case of DPPC molecules, all carbon atoms of methylene and methyl groups with non-polar hydrogens are treated as united atoms. A MD force force-field and an initial configuration of a hydrated DPPC bilayer was taken from ref [54]. The Simple Point Charge (SPC) model [55] was used for water. The force-field used for the azaaromatic molecules was parameterized according to the equilibrium DFT-optimized structure and electronic charges [7]. This force-field was previously adopted to the GROMOS96 force-field and it is tested to reproduce hydrogen bonding behavior of these compounds in bulk water and in mixed *n*-hexane/water solutions, as described in our previous study [7]. The distribution of azaaromatic probes within a model membrane was modeled for a lipid bilayer, existing in the biorelevant liquid crystalline phase, so that the simulation temperature was chosen as 323 K. At the beginning of MD simulations, the whole system was pre-equilibrated for 2 ns at the constant number of particles, constant pressure, P=1 atm, and the constant temperature, T=323 K (NPT ensemble). Three-dimensional periodic boundary conditions were applied with the z axis lying along

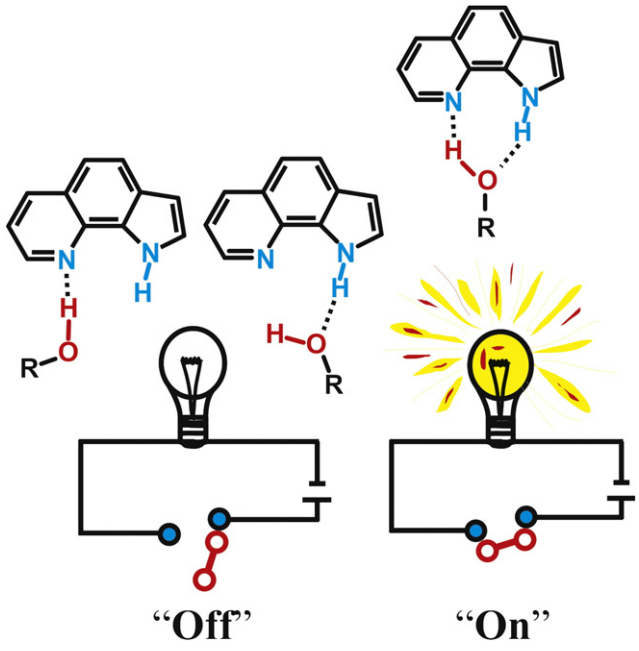

Fig. 2. Operating principle of "off–on" fluorescence signaling by solvent-assisted excited-state proton transfer.

a direction normal to the bilayer. The pressure was controlled semi-isotropically, so that the x–y and z sizes of the simulation box were allowed to fluctuate independently from each other, keeping the total pressure constant. Thus, membrane area and thickness were therefore free to adjust under the NPT condition. The reference temperature and pressure were kept constant using a weak coupling scheme [56] with coupling constant of $\tau_p = 0.1$ ps for temperature coupling and $\tau_t = 1.0$ ps for pressure coupling. Electrostatic interactions were simulated with the particle mesh Ewald (PME) [57] approach using the long-range cutoff of 1.8 nm. The cutoff distance of Lennard-Jones interactions was also equal to 1.8 nm. This MD setup has been demonstrated to be optimal for the simulations of the equilibrium properties of a DPPC bilayer [58]. All bond lengths in DPPC and the solute molecules were kept constant using the LINCS routine [59]. The integration time step was 2 fs. The MD simulations were carried out using GROMACS set of programs, version 3.0 [60].

3. Results and discussion

3.1. Bilayer structure

One of the most important structural parameters which describe packing of phospholipid molecules within a bilayer is the surface area per one lipid molecule. This parameter characterizes the bilayer structure and, therefore, it is commonly used to ensure that an adequate bilayer model and force force-fields are employed in MD simulations. In the case of our MD simulations of a fully hydrated DPPC bilayer in pure water at $T = 323$ K, we estimated the average value of the surface area per lipid to be equal to 64 ± 1 Å^2 per one molecule. The calculated area agrees well with the experimental value of 62.9 Å^2 for a liquid crystalline DPPC bilayer [37]. In addition, the MD results for all major structural and dynamics properties of a pure DPPC membrane are also found to be fully consistent with previous MD studies for the same bilayer in the liquid crystalline phase [61]. Due to a low concentration, the influence of the probes on the overall structure of the membrane is found to be small. This conclusion is confirmed by the analysis of regular bilayer properties evaluated for a pure DPPC bilayer and for the bilayer in the presence of the azaaromatic probes. In the presence of the probes, the surface area per lipid is found to be only slightly increased to 65 ± 1 Å^2. Such behavior is consistent with early experimental works in which much higher concentrations of probes of similar chemical nature, indole and tryptophan, have been used. The presence of these probes has been shown to cause only minor structural changes in the lipid bilayers [50].

3.2. Probe distribution at a water/bilayer interface

To gain insight into the partitioning behavior and distribution of PQ, PC and 7AI across the DPPC bilayer, eight molecules of each probe were initially added, in a random fashion, into aqueous solution at the vicinity of the bilayer interface (four probes per each bilayer leaflet). Series of MD equilibration runs of the studied probe/bilayer systems were performed. After that, the process of the probe distribution between aqueous solution at neutral pH and the lipid membrane was studied by the MD simulations. This type of simulations reproduces the passive thermally-driven diffusion of the probes in the periodic simulation box. The initial configuration of a PQ/DPPC system containing eight PQ molecules is shown in Fig. 3.

The MD simulations demonstrate that, during the first 10 ns, a significant fraction of the probes tend to diffuse from aqueous solution into the polar interfacial region of the DPPC bilayer. The distribution of the PQ molecules at the end of the 20 ns simulation is presented in the middle of Fig. 3. Further analysis of time evolution of the PQ/DPPC system shows that when the probe molecules reach the headgroup region of the membrane, the diffusion of the probes slows down dramatically. To illustrate a typical distribution of the PQ probes at the end of the 50 ns simulation period, one selected instantaneous configuration of the PQ/DPPC system is shown in Fig. 3 (*bottom*).

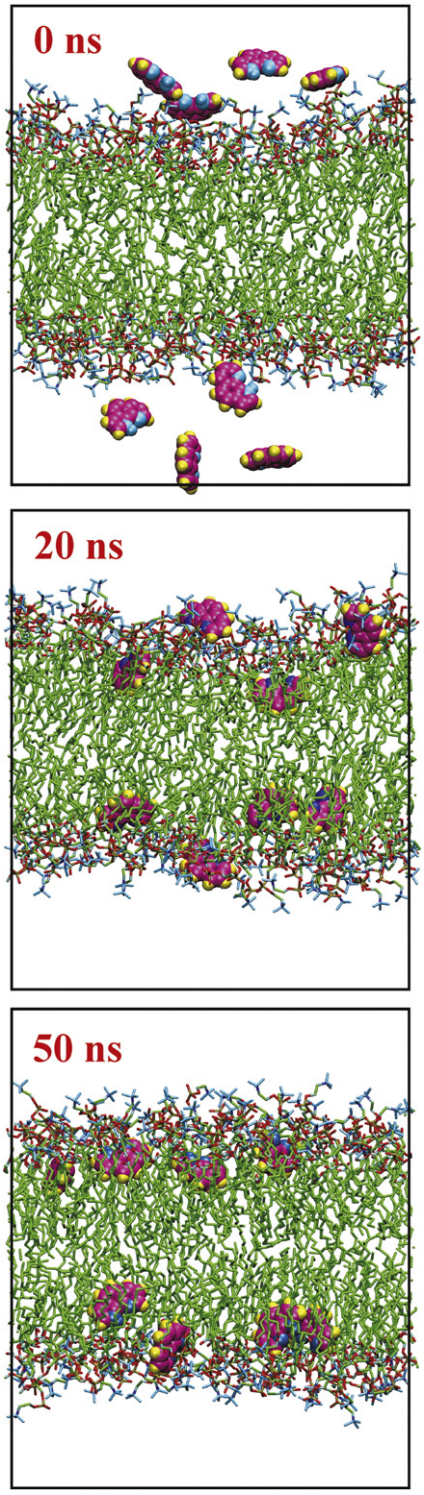

Fig. 3. A snapshot of the MD boxes taken from the simulations of 8 PQ molecules in the DPPC bilayer after 0 ns, 20 ns and 50 ns of the NPT simulation. Water molecules are not shown for clarity. The PQ molecules are rendered with enlarged atomic van der Waals radii.

To evaluate the distribution of PQ, PC and 7AI within the DPPC bilayer quantitatively, we also consider mass density profiles of different molecular components across the bilayer. The position of all atoms in the system were calculated and averaged with respect to the z axis, normal to the bilayer. Using the symmetry of the bilayer, the

mass density profiles were also averaged over the two bilayer leaflets. Fig. 4 shows the mass density profiles of the simulated systems, including water, the DPPC bilayer and the probe molecules. The mass profiles were obtained by averaging the MD trajectory for the last 40 ns of the simulation period. The results for the density distribution of the individual functional groups of the bilayer, such as choline, phosphate and carbonyl groups, as well as a glycerol backbone and acyl chains of the phospholipids, are found to be fully consistent with previous MD simulations for the same bilayer [37,39,58,61]. Fig. 4a–c shows the mass distribution of the probes within the DPPC bilayer. As can be seen, 7AI is distributed throughout the interfacial region to the hydrocarbon acyl chain core of the bilayer, Fig. 4a. In contrast to 7AI, PC shows the localization preference for the hydrocarbon region of the bilayer below the glycerol moiety, Fig. 4c. In the case of PQ, two localization sites at two different depths in the bilayer can be identified; a major site is found to be in the hydrocarbon core and a minor population of PQ is observed at the interface. Thus, the three studied probes demonstrate different localization behavior and the depth in the DPPC bilayer that lead to different number of the binding sites.

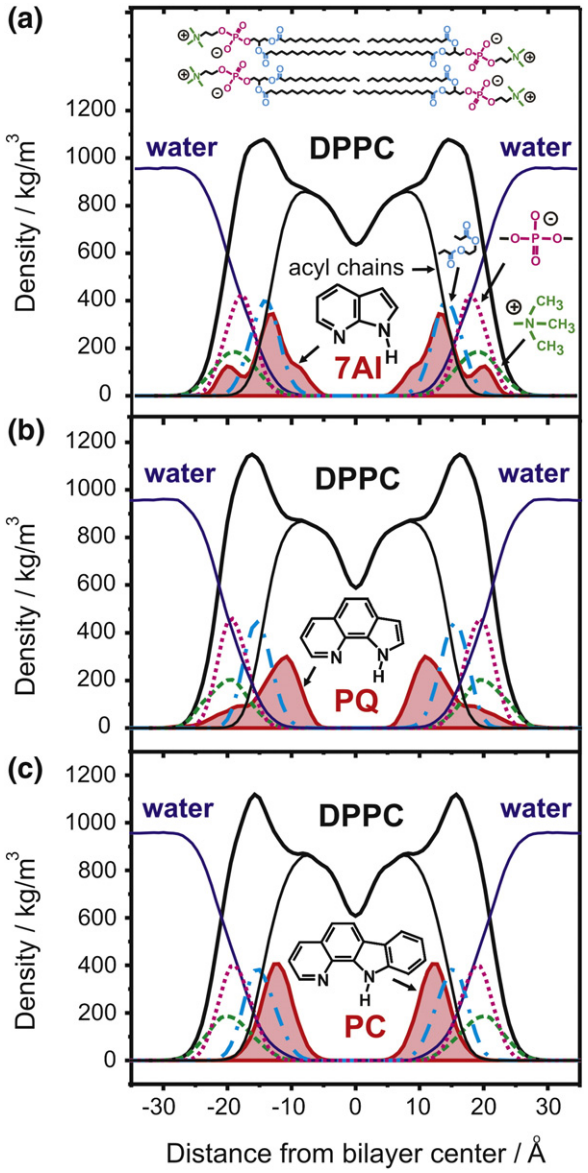

Fig. 4. Mass density distribution profiles for individual components of the DPPC bilayer and for the total density distribution of eight molecules of 7AI (a), PQ (b) and PC (c). All the density profiles are plotted with respect to the center of the *z* axis of the MD box.

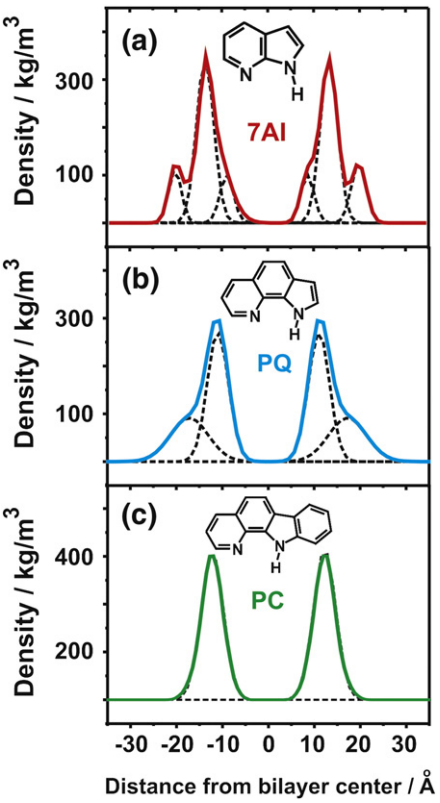

Fig. 5. Comparison of mass density distributions of the probes across the bilayer; dotted lines show a Gaussian decomposition analysis for individual binding sites; 7AI (a), PQ (b) and PC (c).

Comparison and detailed decomposition analysis of individual binding sites for the probes are shown in Fig. 5 and summarized in Table 1. In the case of 7AI, three binding sites *A*, *B* and *C*, in which the population maxima are located at 8.6, 13.3 and 19.8 Å from the bilayer center, may be identified among the broad probe distribution, Fig. 5a. At the same time, PC is characterized by one well-defined binding region with the center at 12.2 Å. In terms of the probe localization, PQ is found to be similar to PC, so that one major deeply deeply-located binding site (*A*) is observed at the depth of 11 Å, Fig. 5b and Table 1. The second broad population (site *B*) is observed at 17.2 Å. Based on these results, it seems that molecular shape and aromaticity of the probes play an important role for the probe localization. The probe location is determined by the hydrophobic effect and, also, by some tendency to drive the aromatic hydrophobic probe out of water. The number of aromatic rings increases in the sequence 7AI–PQ–PC; this leads to the corresponding increase in the hydrophobic character of the probes.

Table 1
Summary of Gaussian decomposition analysis for probe–membrane binding sites

Binding site	7AI				PQ			PC	
	P[a] (%)	Max[b] (Å)	fwhm[c] (Å)	*P* (%)	Max (Å)	fwhm (Å)	*P* (%)	Max (Å)	fwhm (Å)
A	15	8.6	3.0	62	11.0	4.6	100	12.2	4.9
B	65	13.3	3.8	38	17.2	8.3	–	–	–
C	20	19.8	3.3	–	–	–	–	–	–

[a] Population (*P*) of a binding site.
[b] Maximum of a Gaussian band.
[c] Full width at half maximum.

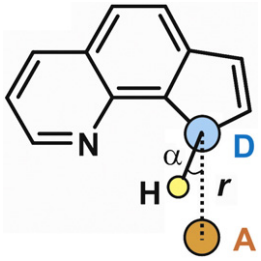

Fig. 6. An example of geometrical criteria ($r \le r_{HB}$=3.5 Å and $\alpha \le \alpha_{HB}$=30°) for hydrogen-bonding between a donor (Don) and an acceptor (Acc) in PQ.

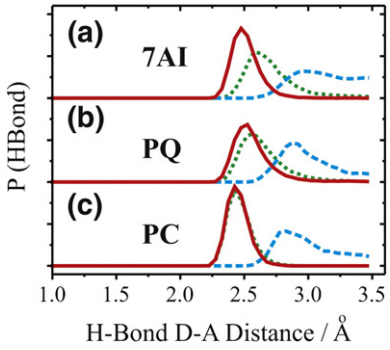

Fig. 7. Distribution of hydrogen bond donor–acceptor distances for 7AI (a), PQ (b) and PC (c). The distance distribution between the donor, the imino nitrogen atom (NH) of the probe molecule (see Fig. 6 for details) and an acceptor, oxygen atoms of a lipid phosphate group is shown by a solid red line; between the donor and oxygen atoms of a lipid glycerol moiety by a dotted green line; between the donor and water oxygen atoms by a dashed blue line.

Therefore, as can be seen in Fig. 4a–c and Fig. 5a–c, the depth of the probe localization in this sequence is gradually shifted deeper inside the hydrocarbon acyl chain core of the bilayer.

In addition, we analyzed the possibility of the penetration of the probes through the bilayer. During our MD analysis, we found that there are no events where the azaaromatic probe is crossing the bilayer from one leaflet to the other.

3.3. Probe–lipid hydrogen bonding

We performed a hydrogen-bonding analysis to determine favorable hydrogen bonds formed between the probes and interfacial water and the DPPC lipids. A hydrogen bond between donor (Don) and acceptor (Acc) atoms is assumed to exist if Don–Acc configuration fulfills certain geometric criteria, such as Don–Acc distance (r_{HB}) and angle (α_{HB}), Fig. 6. An imino nitrogen atom of the probe was chosen as a donor and oxygen atoms of water, phosphate and glycerol groups served as possible hydrogen bond acceptors. Table 2 summarizes the results of the hydrogen-bonding analysis.

Table 2 shows that the majority of 7AI molecules are involved in hydrogen bonds with water and the bilayer lipids, whereas a significant fraction (about 24% and 33%) of PQ and PC, respectively, is found to be hydrogen-bond-free. Due to a large population of 7AI localized on the water–bilayer interface, and, therefore, existing in contact with interfacial water, the relative frequency of the occurrence of 7AI–water hydrogen bonds is estimated to be about 44%. For comparison, as seen in Table 2, the probe–water hydrogen-bonding is gradually decreased for PQ and PC, to be in agreement with the deeper localization of these probes inside the hydrophobic, water-free region of the bilayer, Fig. 4. The distribution of the hydrogen bond distances, r_{HB} is summarized in Table 2 and Fig. 7. The H-bond distance and angle distributions show that all the three probes form the strong hydrogen bond with the oxygen atoms of the lipid phosphate head group, whereas they are interacting weakly with water molecules. It is important to conclude that since the significant population of PQ and PC are found to be hydrogen-bond-free, this indicates that the favorable localization of these probes inside the hydrocarbon core of the bilayer is not driven by hydrogen-bonding.

3.4. Radial-distribution functions

The partial radial distribution functions, $g(R)$, are calculated to study details of interactions of the probes with water and the lipids. The $g(R)$ is therefore used as a complementary tool for the hydrogen boning analysis. The $g(R)$ functions are useful to evaluate whether the probe molecules interact with particular functional groups of the lipids to form hydrogen bonds or whether the overlapping distributions between the bilayer and probes observed in Fig. 4 are due to non-specific van der Waals interactions. Fig. 8 shows the $g(R)$ functions calculated between the NH hydrogen atom of PQ, PC, 7AI and the oxygen atoms of the lipid molecules. Our analysis indicates that the structured features of $g(R)$ are observed between the NH hydrogen atoms and the phosphate or glycerol groups of the lipids. The first peak of $g(R)$ is seen for all the probes at distances 1.5–1.6 Å, Fig. 8a–b. These distances correspond to hydrogen-bonding between the NH hydrogen and the oxygen atoms of the functional groups of the lipids.

3.5. Comparison with indole and its analogues in model membranes

Different spectroscopic techniques have been used in an attempt to describe the average location and orientation of indole and its structural analogues within phospholipid bilayers. Yau et al. [50] have applied a solid-state deuterium NMR spectroscopy to measure the effect of indole and *N*-methylindole on the lipid palmitoyl chain order parameters of a POPC bilayer. The authors have demonstrated that indole probes are preferentially found mostly in the upper acyl chain and headgroup regions of a POPC membrane. Based on induced chemical shifts and deuterium quadrupolar splitting data, it has also been concluded that indole-based azaaromatic probes were usually oriented in a bilayer in

Table 2
Results of the hydrogen-bonding analysis between the probe molecules, lipids, and water

Hydrogen bond type	7AI				PQ				PC			
	F[a] (%)	r_{HB}[b] (Å)	fwhm[c] (Å)	α_{HB}[d] (°)	F[a] (%)	r_{HB}[b] (Å)	fwhm[c] (Å)	α_{HB}[d] (°)	F[a] (%)	r_{HB}[b] (Å)	fwhm[c] (Å)	α_{HB}[d] (°)
NH–water oxygen	44.4	2.98	0.58	11.5	26.8	2.88	0.37	12.0	22.8	2.83	0.42	14.0
NH–phosphate oxygen	39.5	2.49	0.19	5.5	21.8	2.52	0.22	8.5	14.3	2.42	0.17	6.5
NH–glycerol oxygen	10.9	2.60	0.27	6.5	27.3	2.57	0.26	9.0	29.4	2.44	0.16	8.5
No H-bonds	5.2	–	–	–	24.1	–	–	–	33.5	–	–	–

[a] The relative frequency (F) of the occurrence of hydrogen-bonding.
[b] Distribution peak of the H-bond donor–acceptor distance, see Figs. 6 and 7 for details.
[c] Full width at half maximum of the H-bond donor–acceptor distance distribution.
[d] Average H-bond donor–acceptor angle.

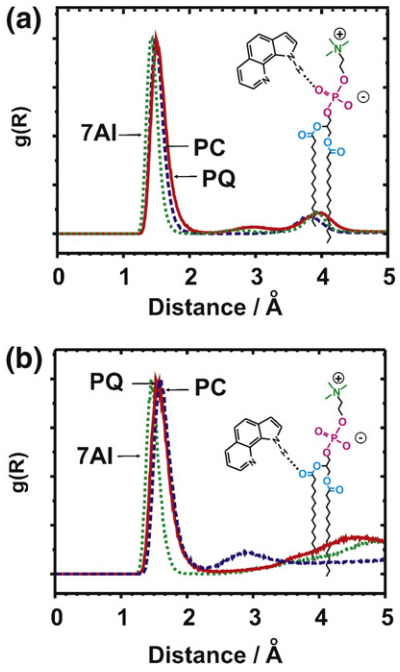

Fig. 8. Radial pair distribution functions $g(R)$ of the N–H hydrogen atom of PQ (solid line), PC (dashed line) and 7AI (dotted line) around the oxygen atoms of the phosphate (a) and glycerol (b) groups of the DPPC lipids. As an example, corresponding hydrogen-bonding between probe and lipid molecules is schematically shown for PQ.

such a way that their aromatic ring plane is aligned parallel to the direction normal to the bilayer. Linear dichroism spectroscopy studies on the orientation of indole electronic transition moments in model membrane has shown that in an intrinsically adopted orientation the indole long axis adopts an angle of 60–65° from the membrane normal [62]. Moreover, the comparison between the partitioning behavior of indole and its *N*-methylated analogue has revealed that the hydrogen-bonding between the imino hydrogen of indole and the phosphate or ester oxygens of lipids might not be primarily responsible for the interfacial location of indole derivatives. An NMR study by Gaede and coworkers has demonstrated that the indole binding location in the lipid environment was driven by many factors, including electrostatic and van der Waals interactions, entropic contributions, and hydrogen bonding [53]. Complex nature of interactions between indole and a lipid membrane has also been suggested by a MD study by Norman and Nymeyer [63]. These authors have found three binding sites for indole in a POPC bilayer; *a*) an interfacial binding site near the glycerol moiety, *b*) a weakly bound interfacial site near the choline group, *c*) a weakly bound site in the middle of the hydrocarbon core of the POPC bilayer. It is interesting to note that, in terms of the localization depth within the lipid membrane, the two major binding sites of 7AI observed in our simulations for the DPPC bilayer are found to be similar to those simulated for indole in POPC. Recent MD simulations by Tieleman's group, using potentials of mean force (PMF) calculations, have also found that partitioning of tryptophan in a DOPC bilayer is characterized by a deep interfacial minimum at 11–13 Å from the bilayer center [64]. Therefore, these PMF calculations also strongly supported the deep interfacial binding of tryptophan with its binding localization to be similar to the major binding site of 7AI, located at 11–12 Å from the DPPC bilayer center.

3.6. Possible applications of studied azaaromatics for monitoring of water content in bilayers

The studied azaaromatic compounds are known to show the hydrogen-bonding-dependent photophysics [1–13,24–29], which open possibilities for their application as water tracers in lipid membranes, Fig. 2. Our MD results for the three different azaaromatic compounds show that their distribution and favorable localizations across the DPPC bilayer are varied due to their different chemical structure, Figs. 4 and 5. 7AI is predicted to have a rather broad distribution across chemically highly heterogeneous bilayer interface, whereas more hydrophobic PQ and PC are more homogeneously localized, favorably below the glycerol moieties of DPPC. However, the major binding population of the studied azaaromatics is still characterized by similar binding fashion, so that the polar nitrogen atoms of the azaaromatics face out of the bilayer hydrocarbon core toward the interfacial water phase. Our MD simulations also show various hydrogen-bonded populations as well as a hydrogen bond free fraction of the probe molecules in the DPPC bilayer, Table 2. In the case of 7AI, about 44% of the whole probe population is expected to be in contact with the interfacial water, whereas in the case of PQ and PC this fraction is decreased to 27% and 23%, (Table 2) respectively. However, our previous MD study have shown that, due to more favorable topology of hydrogen bond donor–acceptor centers, an equilibrium fraction of the "cyclic" complexes formed by PQ in bulk water is actually found to be significantly higher than that of 7AI. Hydrogen-bonding-sensitive fluorescence of the studied azaaromatics allows, in principle, to discriminate between two kinds of hydrogen hydrogen-bonded complexes, termed "cyclic" and "noncyclic", Fig. 2. In the "cyclic" complex, the azaaromatic molecule is hydrogen-bonded in a "cyclic" configuration to a single water molecule. This structure is known to be reactive for the solvent-assisted tautomerization, enabling fluorescence signaling by red-shifted, long-wavelength tautomeric emission. Alternatively, the probe compound may involve hydrogen bonding with water chains or polar lipid groups in "noncyclic" configurations, which are also known to be "blocked" for the solvent-assisted phototautomerization. Therefore, due to the presence of a probe molecule in more than one location in a membrane, some spectral heterogeneity and complex fluorescence dynamics are expected. 7AI is expected to be present in a form of various hydrogen-bonded species located across the bilayer interface. PQ and PC are more homogeneously localized in the deeper part of the bilayer and, therefore, they are expected to be in contact with deeply penetrating interfacial water. The appearance of the characteristic tautomeric red-shifted emission in fluorescence spectra of these compounds, distributed in the lipid membrane, enables monitoring the content and properties of the deeply penetrating water. It would be of practical interest to verify our MD results for fluorescence dynamics of these azaaromatic probes in a lipid environment.

4. Conclusions

The MD simulation study has been carried out to investigate the distribution of fluorescent azaaromatic probes, namely, 1*H*-pyrrolo[3,2-*h*]quinoline (PQ), 11*H*-dipyrido[2,3-*a*]carbazole (PC) and 7-azaindole (7AI) at a water/membrane interface. Our interest has been focused on the favorable binding sites of the probes within a dipalmitoylphosphatidylcholine (DPPC) bilayer. Eight molecules of each probe (four probe molecules per each bilayer leaflet) were used to sample a process of the probe distribution between aqueous solution at neutral pH and the lipid membrane. The probe distribution was simulated by reproducing the thermally-driven passive diffusion. The MD simulations show that a significant fraction of PQ, PC and 7AI molecules tends to diffuse from aqueous solution into the polar interfacial region of the bilayer. PQ and PC are preferentially accommodated in the hydrocarbon core of the bilayer below the glycerol moiety, so that one major deeply-located binding site is observed with the population maximum located at 11–12 Å from the bilayer center. In addition, it has been found that the hydrophobic, aromatic parts of these probes are located inside the hydrophobic acyl chain region of DPPC. In contrast to PQ and PC, 7AI is characterized by a broad distribution between the DPPC interface and water, so that the three preferable binding sites are identified. It has been found that an

increase in the number of aromatic rings in the sequence 7AI–PQ–PC leads to the overall increase in the hydrophobic character of the probes. Therefore, the depth of the probe localization in this sequence is gradually shifted deeper inside the hydrocarbon acyl chain core of the bilayer. The MD simulations reveal that the favorable localizations of the studied azaaromatic probes within the DPPC bilayer are not driven by probe–lipid hydrogen-bonding. The preferable distribution of the probes in the bilayer is adopted by electrostatic dipole–dipole and van der Waals interactions.

References

[1] J. Waluk, Hydrogen-bonding-induced phenomena in bifunctional heteroazaaromatics, Acc. Chem. Res. 36 (2003) 832–838.
[2] J. Herbich, J. Dobkowski, R.P. Thummel, V. Henge, J. Waluk, Intermolecular excited-state double proton transfer in dipyridocarbazole:alcohol complexes, J. Phys. Chem., A 101 (1997) 5839–5845.
[3] A. Kyrychenko, J. Herbich, M. Izydorzak, M. Gil, J. Dobkowski, F.Y. Wu, R.P. Thummel, J. Waluk, Photoinduced double proton transfer: inter- and intramolecular cases, Isr. J. Chem. 39 (1999) 309–318.
[4] A. Kyrychenko, J. Herbich, M. Izydorzak, F. Wu, R.P. Thummel, J. Waluk, Role of ground state structure in photoinduced tautomerization in bifunctional proton donor–acceptor molecules: 1*H*-Pyrrolo[3,2-*h*]quinoline and related compounds, J. Am. Chem. Soc. 121 (1999) 11179–11188.
[5] J.C. del Valle, E. Dominguez, M. Kasha, Competition between dipolar relaxation and double proton transfer in the electronic spectroscopy of pyrroloquinolines, J. Phys. Chem., A 103 (1999) 2467–2475.
[6] D. Marks, H. Zhang, P. Borowicz, J. Waluk, M. Glasbeek, (Sub)picosecond fluorescence upconversion studies of intermolecular proton transfer of dipyrido[2,3-*a*:3',2'-*i*] carbazole and related compounds, J. Phys. Chem., A 104 (2000) 7167–7175.
[7] A. Kyrychenko, Y. Stepanenko, J. Waluk, Molecular dynamics and DFT studies of intermolecular hydrogen bonds between bifunctional heteroazaaromatic molecules and hydroxylic solvents, J. Phys. Chem., A 104 (2000) 9542–9555.
[8] M. Kijak, A. Zielińska, R.P. Thummel, J. Herbich, J. Waluk, Photoinduced double proton transfer in water complexes of 1*H*-pyrrolo[3,2-*h*]quinoline and dipyrido [2,3-*a*:3',2'-*i*]carbazole, Chem. Phys. Lett. 366 (2002) 329–335.
[9] J. Herbich, M. Kijak, R. Luboradzki, M. Gil, A. Zielińska, Y.Z. Hu, R.P. Thummel, J. Waluk, In search for phototautomerization in solid dipyrido[2,3-a:3',2'-*i*] carbazole, J. Photochem. Photobiol., A Chem. 154 (2002) 61–68.
[10] A. Kyrychenko, J. Waluk, Excited-state proton transfer through water bridges and structure of hydrogen-bonded complexes in 1*H*-pyrrolo[3,2-*h*]quinoline: adiabatic time-dependent density functional theory study, J. Phys. Chem., A 110 (2006) 11958–11967.
[11] C.A. Taylor, M.A. El-Bayoumi, M. Kasha, Excited-state two proton tautomerism in hydrogen-bonded N-heterocyclic base pairs, Proc. Natl. Acad. Sci. U. S. A. 63 (1969) 253–260.
[12] P. Avouris, L.L. Yang, M.A. El-Bayoumi, Excited-state interactions of 7-azaindole with alcohol and water, Photochem. Photobiol. 24 (1976) 211–216.
[13] P.-T. Chou, The host/guest type of excited-state proton transfer; a general review, J. Chin. Chem. Soc. 48 (2001) 651–682.
[14] C.-Y. Wei, W.-S. Yu, P.-T. Chou, F.-T. Hung, C.-P. Chang, T.-C. Lin, Conjugated dual hydrogen-bond mediating proton-transfer reaction in 3-hydroxyisoquinoline, J. Phys. Chem., B 102 (1998) 1053–1064.
[15] P.-T. Chou, C.-Y. Wei, C.R.C. Wang, F.-T. Hung, C.-P. Chang, Proton-transfer tautomerism of 7-hydroxyquinolines mediated by hydrogen-bonded complexes, J. Phys. Chem., A 103 (1999) 1939–1949.
[16] J.D. Geerlings, C.A.G.O. Varma, Active participation of solvent molecules in photoinduced enol-keto tautomerisation of 7-hydroxyquinoline with a mobile proton carrier as substituent, J. Photochem. Photobiol., A Chem. 129 (1999) 129–135.
[17] S. Kohtani, A. Tagami, N. Nakagaki, Excited-state proton transfer of 7-hydroxyquinoline in a non-polar medium: mechanism of triple proton transfer in the hydrogen-bonded system, Chem. Phys. Lett. 316 (2000) 88–93.
[18] Y. Matsumoto, T. Ebata, N. Mikami, Structure and photoinduced excited state keto-enol tautomerization of 7-hydroxyquinoline-$(CH_3OH)_n$ clusters, J. Phys. Chem., A 106 (2002) 5591–5599.
[19] C. Tanner, M. Thut, A. Steinlin, C. Manca, S. Leutwyler, Excited-state hydrogen-atom transfer along solvent wires: water molecules stop the transfer, J. Phys. Chem., A 110 (2006) 1758–1766.
[20] O.H. Kwon, T.G. Kim, Y.S. Lee, D.J. Jang, Biphasic tautomerization dynamics of excited 7-hydroxyquinoline in reverse micelles, J. Phys. Chem., B 110 (2006) 11997–12004.
[21] G. Angulo, J.A. Organero, M.A. Carranza, A. Douhal, Probing the behavior of confined water by proton-transfer reactions, J. Phys. Chem., B 110 (2006) 24231–24237.
[22] J. Herbich, J. Waluk, R.P. Thummel, C.Y. Hung, Mechanisms of fluorescence quenching by hydrogen-bonding in various azaaromatics, J. Photochem. Photobiol., A Chem. 80 (1994) 157–160.
[23] J. Herbich, C.Y. Hung, R.P. Thummel, J. Waluk, Solvent controlled excited-state behavior: 2-(2'-pyridyl) indoles in alcohols, J. Am. Chem. Soc. 118 (1996) 3508–3518.
[24] A. Kyrychenko, J. Herbich, F. Wu, R.P. Thummel, J. Waluk, Solvent-induced *syn-anti* rotamerization of 2-(2'-pyridyl) indole and the structure of its alcohol complexes, J. Am. Chem. Soc. 122 (2000) 2818–2827.
[25] Z. Smedarchina, W. Siebrand, A. Fernández-Ramos, L. Gorb, J. Leszczynski, A direct-dynamics study of proton transfer through water bridges in guanine and 7-azaindole, J. Chem. Phys. 112 (2000) 566–573.
[26] A. Fernández-Ramos, Z. Smedarchina, W. Siebrand, M. Zgierski, Dynamics of the water-catalyzed phototautomerization of 7-azaindole, J. Chem. Phys. 114 (2001) 7510–7526.
[27] Y. Nosenko, M. Kunitski, R.P. Thummel, A. Kyrychenko, J. Herbich, J. Waluk, C. Riehn, B. Brutschy, Detection and structural characterization of clusters with ultrashort-lived electronically excited states: IR absorption detected by femtosecond, J. Am. Chem. Soc. 128 (2006) 10000–10001.
[28] Y. Nosenko, A. Kyrychenko, R.P. Thummel, J. Waluk, B. Brutschy, J. Herbich, Fluorescence quenching in cyclic hydrogen-bonded complexes of 1*H*-pyrrolo[3,2-*h*] quinoline with methanol: cluster size effect, Phys. Chem. Chem. Phys. 9 (2007) 3276–3285.
[29] Y. Nosenko, M. Kunitski, C. Riehn, R.P. Thummel, A. Kyrychenko, J. Herbich, J. Waluk, B. Brutschy, Separation of different hydrogen-bonded clusters by femtosecond UV-ionization-detected infrared spectroscopy: 1*H*-pyrrolo[3,2-*h*] quinoline:$(H_2O)_{n=1,2}$ complexes, J. Phys. Chem., A 112 (2008) 1150–1156.
[30] A. Chattopadhyay, S. Mukherjee, Red edge excitation shift of a deeply embedded membrane probe: implications in water penetration in the bilayer, J. Phys. Chem., B 103 (1999) 8180–8185.
[31] Ira, G. Krishnamoorthy, Probing the link between proton transport and water content in lipid membranes, J. Phys. Chem., B 105 (2001) 1484–1488.
[32] A.S. Klymchenko, G. Duportail, A.P. Demchenko, Y. Mély, Bimodal distribution and fluorescence response of environment-sensitive probes in lipid bilayers, Biophys. J. 86 (2004) 2929–2941.
[33] A.S. Klymchenko, Y. Mély, A.P. Demchenko, G. Duportail, Simultaneous probing of hydration and polarity of lipid bilayers with 3-hydroxyflavone fluorescent dyes, Biochim. Biophys. Acta 1665 (2004) 6–19.
[34] A.K. Lala, Fluorescent and photoactivable probes in depth-dependent analysis of membranes, Chem. Phys. Lipids 116 (2002) 177–188.
[35] O. Maier, V. Oberle, D. Hoekstra, Fluorescent lipid probes: some properties and applications (a review), Chem. Phys. Lipids 116 (2002) 3–18.
[36] P. Jurkiewicz, J. Sýkora, A. Olżyńska, J. Humpoličkova, M. Hof, Solvent relaxation in phospholipid bilayers: principles and recent applications, J. Fluoresc. 15 (2005) 883–893.
[37] D.P. Tielaman, S.J. Marrink, H.J.C. Berendsen, A computer perspective of membranes: molecular dynamics studies of lipid bilayer systems, Biochim. Biophys. Acta 1331 (1997) 235–270.
[38] J. MacCallum, D.P. Tieleman, Computer simulation of the distribution of hexane in a lipid bilayer: spatially resolved free energy, entropy, and enthalpy profiles, J. Am. Chem. Soc. 128 (2005) 125–130.
[39] D.P. Tieleman, Computer simulations of transport through membranes: passive diffusion, pores, channels and transporters, Proceedings of Australian Physiological Society, vol. 37, 2006, pp. 15–27.
[40] J. Ulander, A.D.J. Haymet, Permeation across hydrated DPPC lipid bilayers: simulation of the titrable amphiphilic drug valproic acid, Biophys. J. 85 (2003) 3475–3484.
[41] T.-X. Xiang, B.D. Anderson, Liposomal drug transport: a molecular perspective from molecular dynamics simulations in lipid bilayers, Adv. Drug Deliv. Rev. 58 (2006) 1357–1378.
[42] B. Hoff, E. Strandberg, A.S. Ulrich, D.P. Tieleman, C. Posten, ^{2}H-NMR study and molecular dynamics simulation of the location, alignment, and mobility of pyrene in bilayers, Biophys. J. 88 (2005) 1818–1827.
[43] J. Čurdová, P. Čapková, J. Plášek, J. Repáková, I. Vattulainen, Free pyrene probes in gel and fluid membranes: perspective through atomistic simulations, J. Phys. Chem., B 111 (2007) 3640–3650.
[44] R.D. Kaiser, E. London, Location of diphenylhexatriene (DPH) and its derivatives within membranes: comparison of different fluorescence quenching analyses of membrane depth, Biochemistry 37 (1998) 8180–8190.
[45] J. Repáková, P. Čapková, J.M. Holopainen, I. Vattulainen, Distribution, orientation, and dynamics of DPH probes in DPPC bilayer, J. Phys. Chem., B 108 (2004) 13438–13448.
[46] D. Bemporad, J.W. Essex, C. Luttmann, Permeation of small molecules through a lipid bilayer: a computer simulation study, J. Phys. Chem., B 108 (2004) 4875–4884.
[47] C.J. Högberg, A. Maliniak, A.P. Lyubartsev, Dynamical and structural properties of charged and uncharged lidocaine in a lipid bilayer, Biophys. Chem. 125 (2007) 416–424.
[48] L. Koubi, M. Tarek, M.L. Klein, D. Scharf, Distribution of halothane in a dipalmitoylphosphatidylcholine bilayer from molecular dynamics calculations, Biophys. J. 78 (2000) 800–811.
[49] L. Koubi, L. Saiz, M. Tarek, D. Scharf, M.L. Klein, Influence of anesthetic and nonimmobilizer molecules on the physical properties of a polyunsaturated lipid bilayer, J. Phys. Chem., B 107 (2003) 14500–14508.
[50] W.M. Yau, W.C. Wimley, K. Gawrisch, S.H. White, The preference of tryptophan for membrane interfaces, Biochemistry 37 (1998) 14713–14718.
[51] A. Grossfield, T.B. Woolf, Interaction of tryptophan analogs with POPC lipid bilayers investigated by molecular dynamics calculations, Langmuir 18 (2002) 198–210.
[52] A. Chattopadhyay, A. Arora, D.A. Kelkar, Dynamics of a membrane-bound tryptophan analog in environments of varying hydration: a fluorescence approach, Eur. Biophys. J. 35 (2005) 62–71.
[53] H.C. Gaede, W.M. Yau, K. Gawrisch, Electrostatic contributions to indole–lipid interactions, J. Phys. Chem., B 109 (2005) 13014–13023.
[54] D.P. Tieleman, H.J.C. Berendsen, Molecular dynamics simulations of a fully hydrated dipalmitoylphosphatidylcholine bilayer with different macroscopic boundary conditions and parameters, J. Chem. Phys. 105 (1996) 4871–4880.
[55] J. Hermans, H.J.C. Berendsen, W.F. van Gunsteren, J.P.M. Postma, A consistent empirical potential for water–protein interactions, Biopolymers 23 (1984) 1513–1518.
[56] H.J.C. Berendsen, J.P.M. Postma, W.F. van Gunsteren, A. Dinola, J.R. Haak, Molecular dynamics with coupling to an external bath, J. Chem. Phys. 81 (1984) 3684–3690.
[57] T. Darden, D. York, L. Pedersen, Particle mesh Ewald: an $N\cdot\log(N)$ method for Ewald sums in large systems, J. Chem. Phys. 98 (1993) 10089–10092.

[58] C. Anézo, A.H. de Vries, H.D. Höltje, D.P. Tieleman, S.J. Marrink, Methodological issues in lipid bilayer simulations, J. Phys. Chem., B 107 (2003) 9424–9433.
[59] B. Hees, H. Bekker, H.J.C. Berendsen, J.G.E.M. Fraaije, LINCS: a linear constraint solver for molecular simulations, J. Comput. Chem. 18 (1997) 1463–1472.
[60] E. Lindahl, B. Hess, D. van der Spoel, GROMACS 3.0: a package for molecular simulation and trajectory analysis, J. Mol. Model. 7 (2001) 306–317.
[61] A.H. de Vries, I. Chandrasekhar, W.F. van Gunsteren, P.H. Hünenberger, Molecular dynamics simulations of phospholipid bilayers: influence of artificial periodicity, system size, and simulation time, J. Phys. Chem., B 109 (2005) 11643–11652.
[62] E.K. Esbjörner, C.E.B. Caesar, B. Albinsson, P. Lincoln, B. Nordén, Tryptophan orientation in model membranes, Biochem. Biophys. Res. Commun. 361 (2007) 645–650.
[63] K.E. Norman, H. Nymeyer, Indole localization in lipid membranes revealed by molecular simulation, Biophys. J. 91 (2006) 2046–2054.
[64] J.L. MacCallum, W.F.D. Bennett, D.P. Tieleman, Distribution of amino acids in a lipid bilayer from computer simulations, Biophys. J. 94 (2008) 3393–3404.